IJPSR (2019), Volume 10, Issue 11 (Research Article)

INTERNATIONAL JOURNAL OF PHARMACEUTICAL SCIENCES AND RESEARCH

Received on 22 February 2019; received in revised form, 18 June 2019; accepted, 24 June 2019; published 01 November 2019

GC- MS ANALYSIS AND *IN-SILICO* DOCKING ANALYSIS OF METHANOLIC EXTRACT OF *FICUS RACEMOSA* BARK

A. Poongothai [*1] and S. Annapoorani [2]

Department of Biochemistry [1], Sacred Heart College (Autonomous), Tirupattur - 635601, Tamil Nadu, India.
Department of Biochemistry [2], Avinashilingam Institute of Home Science and Higher Education for Women, Coimbatore - 641043, Tamil Nadu, India.

Keywords:

Ficus racemosa, ADME, Phytochemical constituents and Anti-tumorigenic efficacy

Correspondence to Author:
Dr. A. Poongothai

Assistant Professor,
Department of Biochemistry,
Sacred Heart College (Autonomous),
Tirupattur - 635601, Tamil Nadu,
India.

E-mail: kumuthaannadurai@gmail.com

ABSTRACT: Indian medicinal plants are considered as a vast source of several pharmacologically active principles and compounds, which are commonly used in home remedies against multiple ailments. Plant secondary metabolites such as alkaloids, tannins, steroids, terpenoids, coumarins and phenolic compounds and their semi-synthetic derivatives continue to play an important role in anticancer drug therapy. Molecular docking is a computational technique that aims to predict how a particular small molecule will stably bind to a target protein. It is an important component of many drug discovery projects when the structure of the protein is available. Although it is primarily used as a virtual screening tool, and subsequently for lead optimization purposes, there are also applications in target identification. To characterize the phytochemical constituents and anti-tumorigenic efficacy of methanolic extract of *Ficus racemosa* bark against cancer target proteins using *in-silico* Glide docking and QikProp panel. The results showed that the presence of phytochemical constituent's namely, flavonoids, steroids, saponins, glycoside, tannins, phenolics, fixed oils and fats and the total 24 phytochemical constituents present in MEFrB identified by GC-MS out of 24 compounds only 2, 4, 5, 10, 18 and 24 compounds were found to be successful in SP docking and these compounds were selected for XP docking. In XP and induced fit docking showed high score for only two compounds. ADME properties of these two compounds in QikProp program showed drug able property, solubility and permeability and also obeyed Lipinski's rule.

INTRODUCTION: Medicinal plants continue to be an important therapeutic aid for alleviating the ailments of humankind. The search for eternal health and longevity and remedies to relieve pain and discomfort drove early man to explore his immediate natural surroundings and led to the use of many plants in the development of a variety of therapeutic agents.

QUICK RESPONSE CODE

DOI: 10.13040/IJPSR.0975-8232.10(11).5179-93

The article can be accessed online on www.ijpsr.com

DOI link: http://dx.doi.org/10.13040/IJPSR.0975-8232.10(11).5179-93

Today, there is a renewed interest in traditional medicine and an increasing demand for more drugs from plant sources. Phytochemicals are non-nutritive plant chemicals that have protective or disease preventive properties. The plant produces these chemicals to protect itself but recent research demonstrates that many phytochemicals can protect humans against diseases. There are many phytochemicals in seeds, fruits, herbs and each works differently.

Molecular docking is a computational technique that aims to predict how a particular small molecule will stably bind to a target protein[1]. *Ficus racemosa* Linn. (Moraceae) is an evergreen, moderate to

large-sized spreading, lactiferous, deciduous tree, without much prominent aerial roots found throughout greater part of India in moist localities and is often cultivated in villages for its edible fruit. *Ficus racemosa* Linn. is a large deciduous tree distributed throughout India, particularly in evergreen forests and moist localities. Different parts of *Ficus racemosa* are traditionally used as fodder, edible and ceremonial. All parts of this plant (leaves, fruits, bark, latex, and sap of the root) are medicinally important in the traditional system of medicine in India. The astringent nature of the bark has been employed as a mouth wash in spongy gum and also internally in dysentery, menorrhagia, and hemoptysis.

Its pharmacological activities are hypoglycemic activity, hypolipidemic activity, wound healing, anti-diarrhoeal, anti-helminthic, anti-oxidant and a probable radioprotector, anti-diuretic, hepatoprotective, analgesic, cardioprotective, anti-ulcer and anti-neoplastic [2].

FIG. 1: *FICUS RACEMOSA* BARK

There is no scientific validation on the extraction, screening, and docking studies on the phytochemical constituents of the medicinal plant *Ficus racemosa* against the anticancer targets. The present study to characterize the phytochemical constituents of methanolic extract of *Ficus racemosa* bark by spectral studies. To characterize the anti-tumorigenic efficacy of phytochemical constituents of methanolic extract of *Ficus racemosa* bark against cancer target proteins using *in-silico* Glide docking and QikProp panel.

MATERIALS AND METHODS:

Collection of Plant Material: *Ficus racemosa* bark was collected from Coimbatore district, Tamil Nadu. The collected plant parts were washed thoroughly in tap water, shade dried and finely powdered. During the herbarium of Department of Botany, Tamil Nadu Agricultural University (BOT-005/2010), Coimbatore, Tamil Nadu, India.

Preparation of Organic Extract of *Ficus racemosa* Bark: Twenty grams of the bark of *Ficus racemosa* was filled individually in the thimble and extracted with 200 ml of methanol using Soxhlet apparatus for 24 h. The extract was then distilled and evaporated to dryness. The concentrated extracts were then accurately weighed and stored in small vials at -20 °C, for further studies.

Preliminary Phytochemical Analysis: The phytochemical screening was performed using standard procedures. The procedures for detection of alkaloids, flavonoids, saponins, phenols, glycosides, tannins, carbohydrates steroids and terpenoids [3, 4, 5]. To predict the mechanism of action of the phytochemical constituents of MEFrB docking analysis was carried out using Glide. **Table 1** shows the tools and software used for *in-silico* studies.

TABLE 1: TOOLS AND SOFTWARES USED FOR *IN-SILICO* STUDIES

Tools and Softwares	Description
Pdb	Tumorigenic and microbial target proteins (1Z2B, 1T69, 1W2N, 1SQ5) downloaded with their corresponding co-crystal ligand
Pdbsum	To identify the active site residues of the target protein
Ligplot	It automatically generates schematic diagrams of protein-ligand interactions for a given PDB file
Glide	Software used for docking studies
Ligprep	To prepare the ligands
QikProp 3.2	Assessment of ADME properties

Active Site Residues of Tumorigenic and Microbial Target Protein: Target-based drug discovery begins with the identification of a potential therapeutic drug target and understanding its role in the disease process. In the current study, Histone deacetylases (HDACs) and Tubulin (MTs),

the two tumorigenic target proteins were chosen. The drug targets for each tumorigenic activity were obtained from RCSB Protein Data Bank (http://www.rcsb.org/pdb/home/home.do) with the following PDB ID Histone deacetylases (1T69), Tublin (1Z2B). The structural details of the target proteins are shown in **Table 2**.

TABLE 2: THE STRUCTURAL DETAILS OF THE TARGET PROTEINS

Structural Details	Tumorigenic targets	
	1T69	1Z2B
Resolution [Å]	2.91	4.10
R-Value	0.249	0.212
R-Free	0.310	0.269
Chains	A	A,B,C,D,E

Construction of Ligand Library: The drug is most commonly an organic small molecule that activates or inhibits the function of a biomolecule such as a protein, which in turn results in a therapeutic benefit to the patient.

In the most basic sense, drug design involves the design of small molecules that are complementary in shape and charge to the bimolecular target to which they interact and therefore will bind to it. About 24 phytochemical constituents identified in GC- MS from MEFrB were docked against the tumorigenic targets. The canonical structure or PDB files of the compounds were used for docking.

Prediction of Active Site Residues of Target Protein: The LIGPLOT program automatically generates schematic 2-D representations of protein-ligand complexes from standard Protein Data Bank file input. The output is a color, or black-and-white, Post Script file giving a simple and informative representation of the intermolecular interactions and their strengths, including hydrogen bonds, hydrophobic interactions, and atom accessibilities.

The program is completely general for any ligand and can also be used to show other types of interaction in proteins and nucleic acids. It was designed to facilitate the rapid inspection of many enzyme complexes but has found many other applications.

The program was carried out by:

- Opening the PDB homepage (http://www.ebi. ac.uk/pdbsum/) and entering the PDB ID (1Z2B and 1T69).
- Selecting the ligand it automatically generates schematic diagrams of protein-ligand interactions.

GLIDE Docking: Maestro is the graphical user interface for all of Schrödinger's products: CombiGlide™, Epik™, Glide™, Impact™, Liaison™, Ligprep™ MacroModel™, Phase™, Prime™, QikProp™, Qsite™, and Strike™. Schrödinger developed state-of-the-art chemical simulation software for use in pharmaceutical, biotechnology, and materials science research. Grid-based Ligand Docking with Energetics (GLIDE) searches for favorable interactions between one or more typically small ligand molecules and a larger receptor molecule usually a protein. Each ligand must be a single molecule, while the receptor may include more than one molecule. GLIDE can be run in rigid or flexible docking modes. The later automatically generates confirmation for each input ligand. The combination of positions and orientation of the ligand relative to the receptor, along with its conformation in flexible docking, is referred to as a ligand pose. **Fig. 2** shows the Maestro workspace.

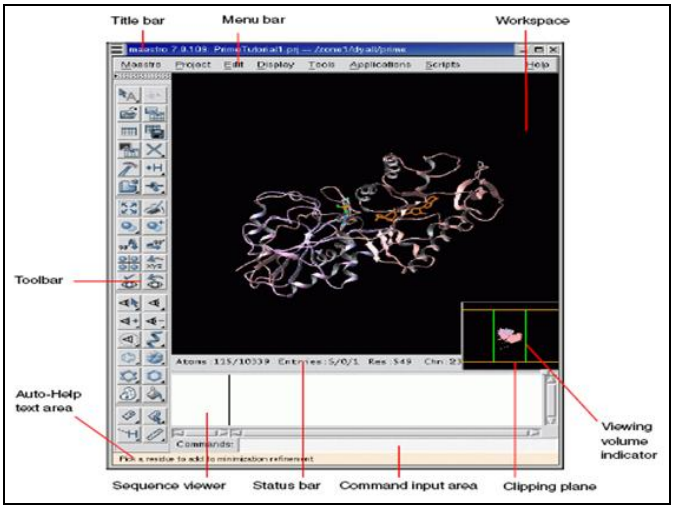

FIG. 2: MAESTRO WINDOW

Running and Monitoring Jobs: Maestro has panels for each product for preparing and submitting jobs. To use these panels, the appropriate product and task from the Applications menu and its submenus should be chosen. Set the appropriate options in the panel, and then click Start to set options for running the job. The Monitor panel is the control panel for monitoring the progress of jobs and for pausing, resuming, or ending jobs. The text pane shows various output

information from the monitored job, such as the contents of the log file. While jobs are running, the Detach, Pause, Resume, Stop, Kill, and Update buttons are active. When no jobs currently running, only the Monitor and Delete buttons are active. When a monitored job ends, the results are incorporated into the project according to the settings used to launch the job.

Preparation of Protein Target Structures: The three-dimensional structures of protein for the selected tumorigenic targets were taken from the PDB (1Z2B and 1T69) and modified for Glide Docking calculations. For Glide calculations, corresponding proteins complex with ligand was imported to Maestro (Schrödinger) and were refined using the Amber force field. The protein contains many chains. Only the chain that is in complex with the ligand will be prepared for further process, and the other chains were deleted.

Preparation of Ligand Compounds: All the 24 phytochemical constituents of MEFrB were the ligand molecules to be docked into the active site of target proteins. The structures of all the small ligand molecules were drawn using the builder panel available in the Schrödinger software. The structures were then energy minimized using the OPLS-2005 force field until it reaches the RMSD 0.0018 Kcal/mol.

Grid Generation: Glide searches for favorable interactions between one or more typically small ligand molecules and a typically larger receptor molecule usually a protein. Each ligand must be a single molecule, while the receptor may include more than one molecule that is a protein and a cofactor. Choose the Receptor Grid Generation from the Glide submenu of the Applications menu. The Receptor Grid Generation panel has three tabbed folders to specify settings for the receptor grid generation job such as a) receptor b) site and c) constraints. To specify the receptor grid for the docking job, click Browse in the Receptor grid section of the Settings folder to open a file selector and choose a grid file (.grd). The file name, without the .grd extension, is displayed in the Receptor grid base name text box.

Protein-Ligand Docking: The Three types of Docking Algorithms used for the current studies are (i) Standard Precision (SP) docking, (ii) Extra Precision (XP) docking and (iii) Induced Fit (IF) docking. In the current study, ligands were docked using all three types of docking. The SP docking is appropriate for screening ligands of unknown quality in large numbers.

The XP docking and scoring is a more powerful and discriminating procedure, which takes longer to run than SP. XP docking is designed to be used on ligand poses that have a high score using SP docking. It used to perform the more expensive docking simulation on worthwhile poses. The IF docking allows the receptor to alter its binding sites so that it more closely conforms to the shape and binding mode of the ligand.

Docking Output Job Files:

Jobname_lig.mae: The input ligand structure file

Jobname_lig_prep.mae: The post preparation ligand structure file

Jobname_lig_ref.mae: The post-refinement ligand structure file, if present, the Receptor structure file contains only the receptor file.

Jobname_prot.mae: The input receptor structure files.

Jobname_prot_prep.mae: The post preparation receptor structure file

Jobname_prot_ref.mae: The post-refinement receptor structure file. Contains the Receptor and ligand structure unless there is a separate Ligand structure file

Jobname.log: The log files for the complete preparation and Refinement job.

Assessment of ADME Properties: The increase in the number of new structures generated each year has not resulted in the expected increase in the number of marketed new drugs. Nearly 40% of drug candidates fail in clinical trials due to poor ADME (Absorption, Distribution, Metabolism, and Excretion) properties. The ability to detect problematic candidates early can dramatically reduce the amount of wasted time and resources.

Qikprop 3.2 Analysis: The QikProp 3.2 efficiently evaluates pharmaceutically relevant ADME

properties for over half a million compounds per hour, making it an indispensable lead generation and lead optimization tool.

Phytochemical Constituents of MEFrB by *in-silico* Studies: Phytochemistry is the branch of chemistry that deals with the isolation and characterization of the available primary and secondary metabolites in plants using the modern techniques like GC-MS and *in-silico* studies. Secondary metabolites play an important role as antioxidants and anti-tumorigenic agents.

Preliminary Phytochemical Analysis: In the present investigation, preliminary phytochemical screening has been done in the MEFrB. The extracts showed the presence of phytochemical constituent's namely, flavonoids, steroids, saponins, glycoside, tannins, phenolics, fixed oils and fats **Table 3**.

Gas Chromatography –Mass Spectroscopy (GC-MS): The major constituents of MEFrB were analyzed using GC-MS analysis. The GC-MS analysis revealed several peaks for MEFrB and identified by matching the peaks with the National Institute of Standards and Technology spectral library. The 24 phytochemical constituents present in MEFrB identified by GC-MS are listed in **Table 4**.

TABLE 3: PHYTOCHEMICAL CONSTITUENTS OF MEFrB

Phytochemical constituents	*Ficus racemosa* bark
Flavonoids	+
Steroids	+
Saponins	–
Glycosides	+
Tannins	+
Phenolics	+
Fixed oils	+
Fats	+

+ indicates presence, - indicates absence

TABLE 4: PHYTOCHEMICAL CONSTITUENTS OF MEFrB IDENTIFIED BY GC-MS ANALYSIS

S. no.	Retention time	Compound name	Molecular formula	Molecular weight	Area %
1	5.43	(S)-2-Benzyloxycarbonylamino-4-oxo-4-phenylbutanoyl azetidine	$C_{21}H_{22}N_2O_4$	366	0.76
2	5.43	1-[N (Benzyloxycarbonyl)aminomethyl]benzotriazole	$C_{15}H_{14}N_4O_2$	282	0.76
3	5.43	Benzyl propenoate	$C_{10}H_{10}O_2$	162	0.76
4	33.71	(Z)-(2S,3S)-2,3-bis[(methoxymethyl)oxy]-5-(4-methoxyphenyl) pent-4-enol	$C_{16}H_{24}O_6$	312	0.80
5	33.71	(E)-(2S,3S)-2,3-bis[(methoxymethyl)oxy]-5-(4-methoxyphenyl) pent-4-enal	$C_{16}H_{22}O_6$	310	0.80
6	32.70	bis(2-ethylhexyl) phthalate	$C_{24}H_{38}O_4$	390	0.77
7	32.70	i-Propyl 3-(phenylamino)-2-(phenylseleno)-3-(phenyl)propanoate	$C_{24}H_{25}NO_2Se$	439	0.77
8	32.70	1,2-Benzenedicarboxylic acid, dicyclohexyl ester	$C_{20}H_{26}O_4$	330	0.88
9	23.52	1-methoxy-5-methyl-1-phenylhex-4-ene	$C_{14}H_{20}O$	204	1.20
10	24.03	1-Hexyl-2-nitrocyclohexane	$C_{12}H_{23}NO_2$	213	0.95
11	30.73	2,2-Diphenyl-1(4-methoxyphenyl)1,2-dihydroazeto[2,1-b] quinazolin-8-one	$C_{29}H_{22}N_2O_2$	430	4.20
12	30.73	(2S)-2-(-2,3-Dimethoxyphenyl)carbonylamino-N-(2,3-dimethoxy benzyl)-3 methylbutylamide	$C_{23}H_{30}N_2O_6$	430	4.20
13	28.72	13-Carbethoxy-12-carbethoxymethyl-pyrrolo[1,2-a:4,3-b']diquinoline-14-ium-chloride	$C_{26}H_{23}ClN_2O_4$	462	0.84
14	28.72	2-(1-ethyl-1-butenyl)-1-nitrocyclohexane	$C_{12}H_{21}NO_2$	211	0.84
15	32.70	1,2-Benzenedicarboxylic acid, dioctyl ester	$C_{24}H_{38}O_4$	390	0.88
16	32.70	1,2-Benzenedicarboxylic acid, disooctyl ester	$C_{24}H_{38}O_4$	390	0.88
17	32.70	i-Propyl 3-(phenylamino)-2-(phenylseleno)-3-(phenyl)propanoate	$C_{24}H_{25}NO_2Se$	439	0.77
18	23.52	Di-isodecyl phthalate	$C_{28}H_{46}O_4$	446	1.05
19	20.86	Methyl 4-Phenyl-3-oxahept-6-enoate	$C_{13}H_{16}O_3$	220	4.46
20	20.86	1-Methyl-2-methyleneacenaphthene-1-carboxaldehyde	$C_{15}H_{12}O$	208	4.46
21	26.21	Pentadecanoic acid,methyl ester	$C_{16}H_{32}O_2$	256	3.73
22	7.77	Undecane, 2-methyl	$C_{12}H_{26}$	170	1.57
23	26.95	11,14, 17- Eicosatrienoic acid, methyl ester	$C_{21}H_{36}O_2$	320	6.85
24	32.71	(+) – Cis – (1S, 4R)-4- (Tetrahydropyran – 2-yloxy)cyclohex – 2- enol	$C_{11}H_{18}O_3$	198	1.27

Active Site Residues of Tumorigenic Target Proteins: The ligplot automatically generates schematic diagrams of protein-ligand interactions for a given PDB file. The **Fig. 3** depicts the active site residues and interactions of co-crystal ligands SHH and VLB with tumorigenic target proteins (1T69 and 1Z2B).

Glide Docking: In GLIDE the crystal structure of various target protein complexes with the ligand is downloaded from Protein Data Bank (PDB ID-1T69 and 1Z2B) and saved.

The downloaded protein is imported into the Maestro workspace and water molecules are deleted and energy minimization procedures were performed for all the target proteins and the four ligand compounds. All the 24 bioactive compounds of MEFrB **Fig. 3**, **4**, **5**, **6** and **7** were chosen for the docking studies.

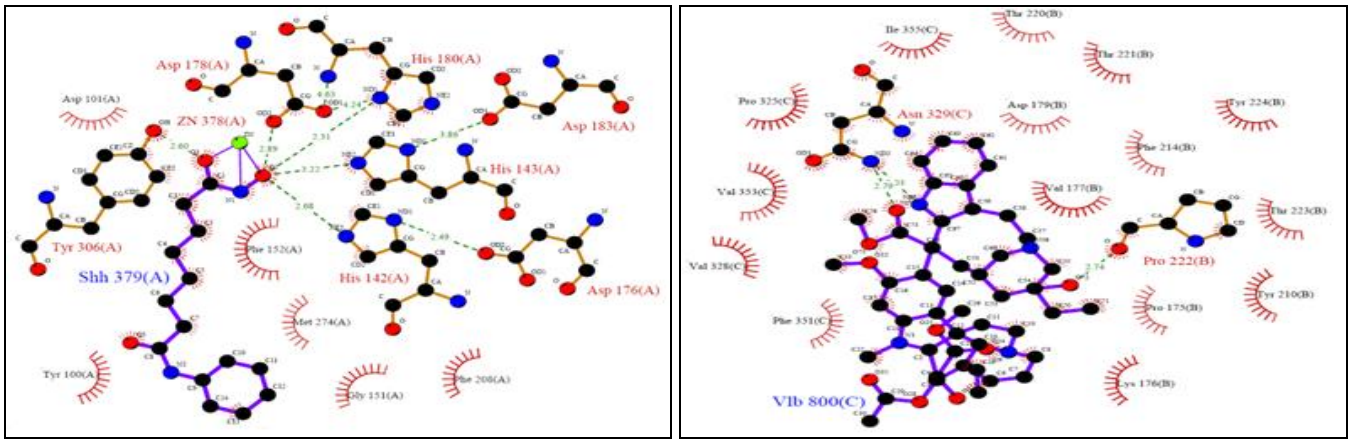

Histone deacetylase (1T69) with co-crystal (SHH) **Tubulin (1Z2B) with co-crystal (VLB)**

FIG. 3: LIGPLOT INTERACTIONS OF TUMOR TARGET PROTEINS AND THEIR ACTIVE SITES

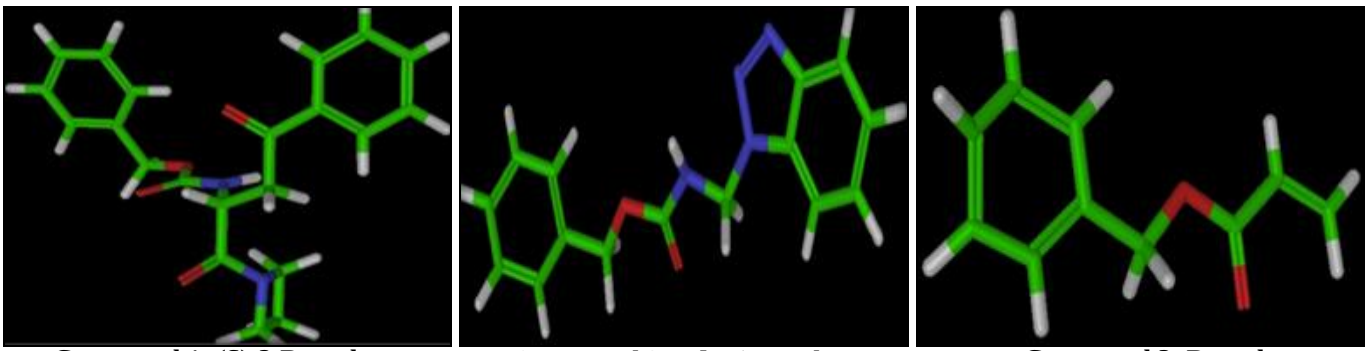

Compound 1: (S)-2-Benzyloxy-carbonylamino-4-oxo-4-phenyl butanoyl azetidine

Compound 2: 1-[N-(Benzyloxy-carbonyl)aminomethyl] benzotriazole

Compound 3: Benzyl propenoate

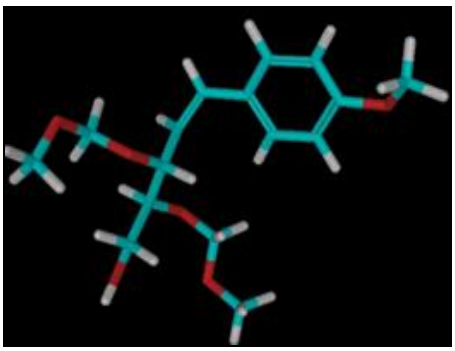

Compound 4: ((Z)-(2S, 3S)-2,3-bis[(methoxymethyl)oxy]-5-(4-methoxyphenyl) pent-4-enol

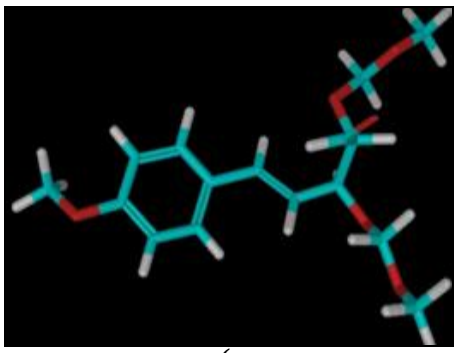

Compound 5: (E)-(2S, 3S)-2,3-bis[(methoxymethyl)oxy]-5-(4-methoxyphenyl) pent-4-enal

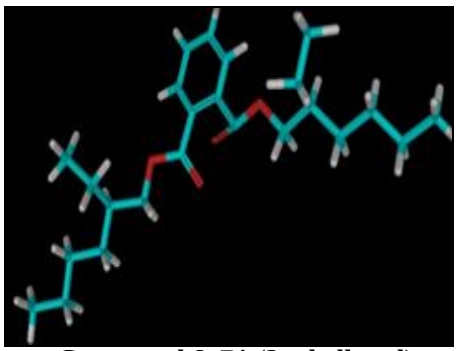

Compound 6: Bis(2-ethylhexyl) phthalate

FIG. 4: STRUCTURE OF BIOACTIVE COMPOUNDS OF MEFrB

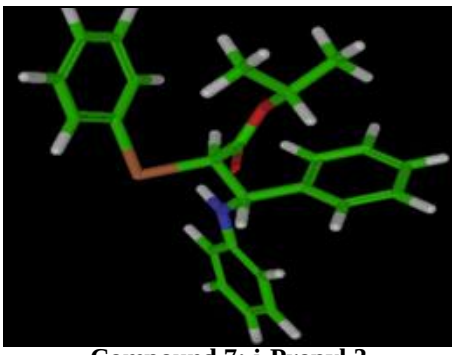

Compound 7: i-Propyl 3-(phenylamino)-2-(phenylseleno)-3-(phenyl)propanoate

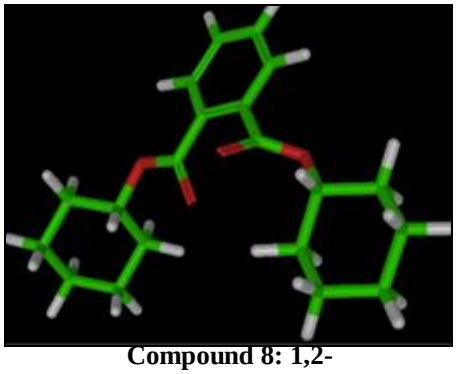

Compound 8: 1,2-Benzenedicarboxylic acid, dicyclohexyl ester (CAS)

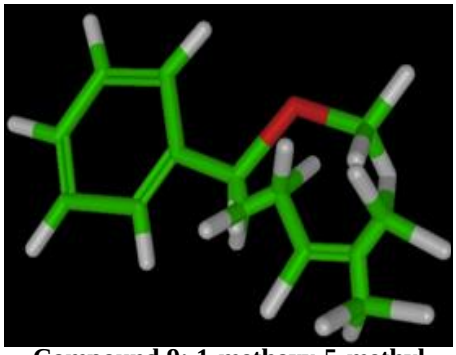

Compound 9: 1-methoxy-5-methyl-1-phenylhex-4-ene

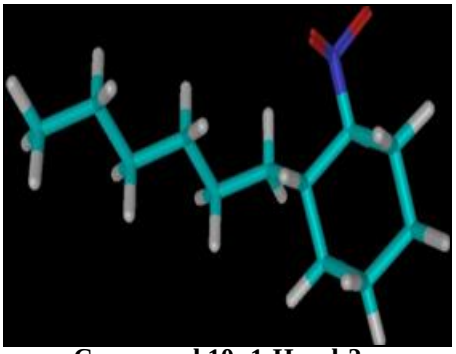

Compound 10: 1-Hexyl-2-nitrocyclohexane

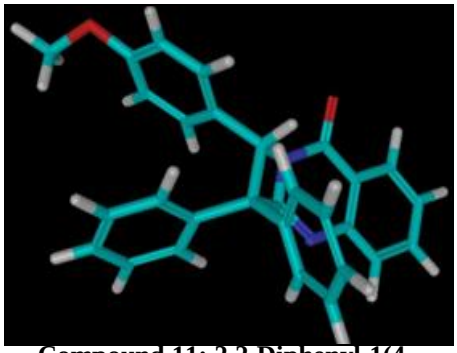

Compound 11: 2,2-Diphenyl-1(4-methoxyphenyl)1, 2-dihydro-azeto[2,1-b] quinazolin-8-one

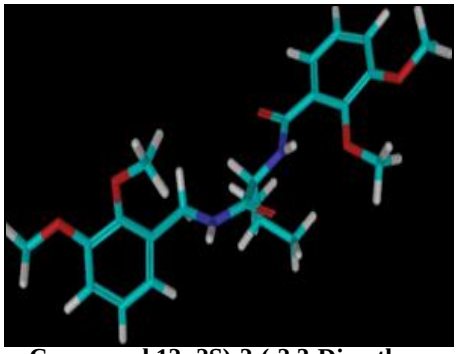

Compound 12: 2S)-2-(-2,3-Dimetho-xyphenyl)carbonylamino-N-(2, 3-di-methoxy benzyl)-3 methylbutylamide

FIG. 5: STRUCTURE OF BIOACTIVE COMPOUNDS OF MEFrB

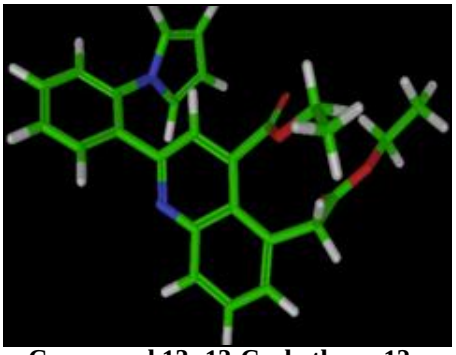

Compound 13: 13-Carbethoxy-12-carbethoxymethyl-pyrrolo [1, 2-a: 4,3-b']diquinoline-14-ium-chloride

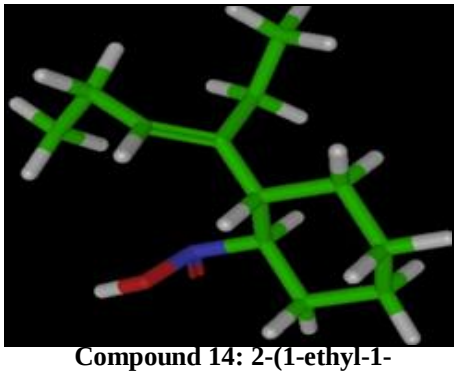

Compound 14: 2-(1-ethyl-1-butenyl)-1-nitrocyclohexane

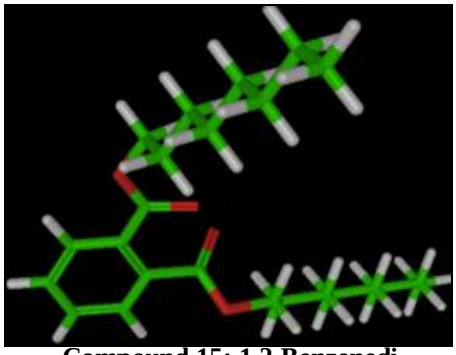

Compound 15: 1,2-Benzenedi-carboxylic acid, dioctyl ester (CAS)

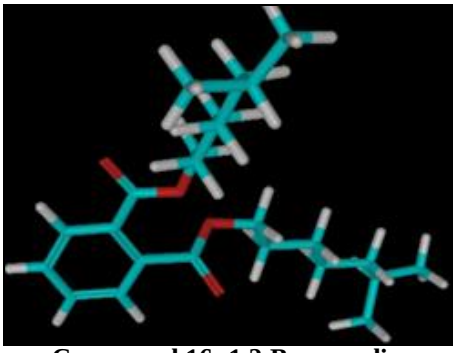

Compound 16: 1,2-Benzenedi-carboxylic acid, diisooctyl ester

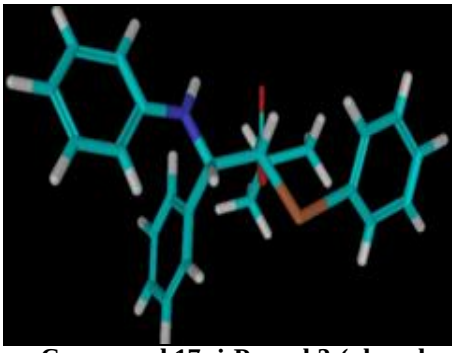

Compound 17: i-Propyl 3-(phenyl amino)-2-(phenylseleno)-3-(phenyl)propanoate

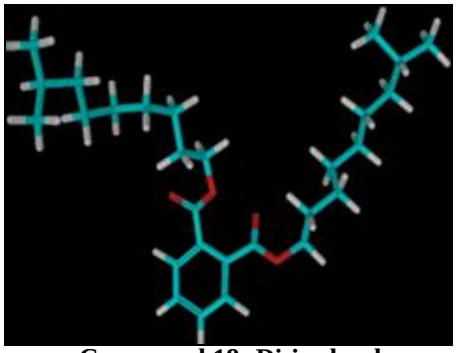

Compound 18: Di-isodecyl phthalate

FIG. 6: STRUCTURE OF BIOACTIVE COMPOUNDS OF MEFrB

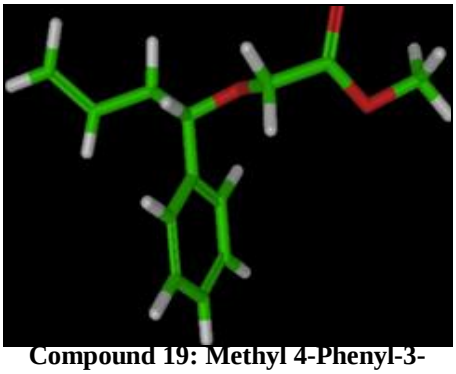

Compound 19: Methyl 4-Phenyl-3-oxahept-6-enoate

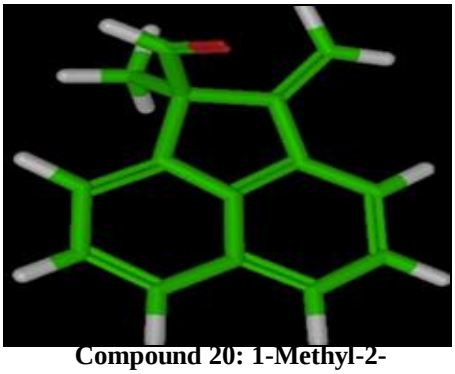

Compound 20: 1-Methyl-2-methyleneacenaphthene-1-carboxaldehyde

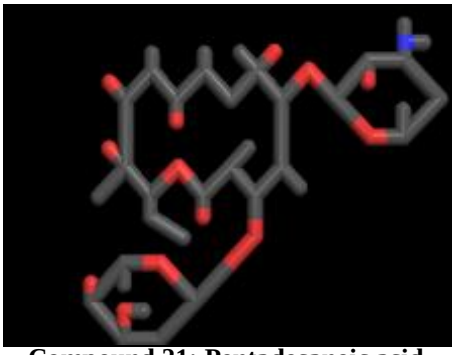

Compound 21: Pentadecanoic acid, methyl ester

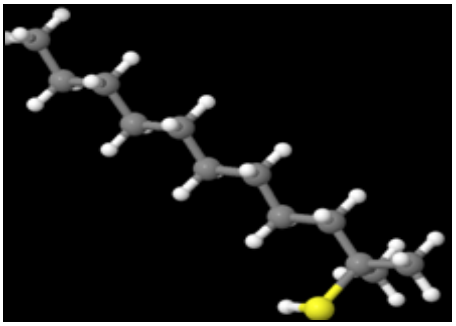

Compound 22: Undecane, 2-methyl

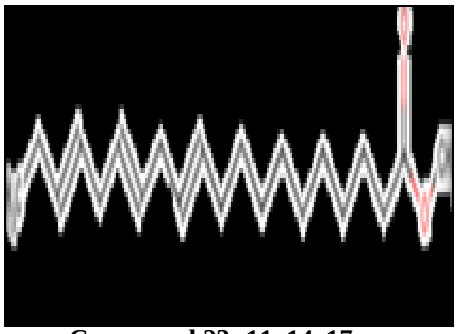

Compound 23: 11, 14, 17-Eicosatrienoic acid, methyl ester

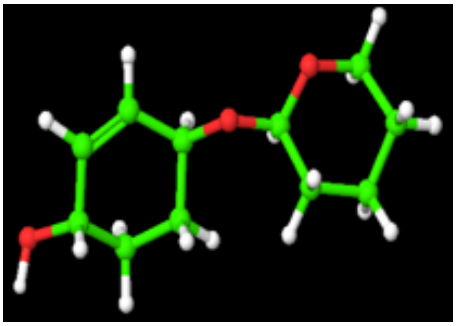

Compound 19: (+) – Cis – (1S, 4R)-4-(Tetrahydropyran – 2- yloxy) cyclohex – 2- enol

FIG. 7: STRUCTURE OF BIOACTIVE COMPOUNDS OF MEFrB

SP Docking: First, all the prepared ligands were subjected to SP docking with all the four target proteins. Based on glide score, glide energy and number of hydrogen bonds, the best ligands can be identified in comparison with corresponding co-crystal ligand (1T69-SHH and 1Z2B-VLB). All the 24 compounds were selected for SP docking. Among the 24 compounds docked with histone deacetylase (1T69) were shown in **Table 5**. Similar steps followed for rest of the 1Z2B target proteins.

TABLE 5: SP DOCKING FOR TUMOR TARGET PROTEIN HISTONE DEACTYLASE (1T69) WITH BIOACTIVE COMPOUNDS OF MEFrB

Tumor targets	Compound number	Glide score	Glide energy (Kcal / Mol)	Hydrogen bond interactions (DH…A)	Bond distance (Å)
Histone deactylase (1T69)	**Co-crystal (SHH)**	**-5.756641**	**-35.742488**	**Asp101(OH…O)**	**2.735**
				Asp 101(NH…O)	**3.009**
	Compound 2	-7.035352	-41.400277	Tyr 306(OH...O)	2.917
				NH…O(Gly 151)	3.074
	Compound 4	-5.320918	-37.999418	Tyr 306(OH...O)	2.662
				Phe 208(NH...O)	2.812
	Compound 5	-5.133904	-33.495655	Tyr 306(OH...O)	2.732
				Phe 208(NH...O)	2.983
	Compound 10	-5.330918	-31.641964	Tyr 302(OH...O)	2.701
				Phe 199 (NH...O)	2.886
	Compound 18	-5.226839	-45.906771	Tyr 298(OH...O)	2.644
				Phe 192(NH...O)	2.902
	Compound 24	-6.727805	-30.855328	Tyr207 (OH….O)	2.345

The SP docking for Histone deacetylase (1T69) with top 24 compounds selected from SP docking, showed six best compounds (4, 5, 10, 18 and 24) in comparison with co-crystal ligand (SHH). The co-crystal ligand showed highest score of -5.756641 showing two strong interactions with the residues Asp 101 and Asp 101 having hydrogen bonds of length 2.735 Å and 3.009 Å. The compound 2 showed highest score of -7.035352 greater than co-crystal showing strong interaction with the residues

Tyr 306 and Gly 151 having hydrogen bonds of length 2.917 Å and 3.074Å. The compound 24 showed highest score of -6.72 7805 greater than co-crystal showing strong interaction with the residues Tyr 207 having hydrogen bonds of length 2.345 Å. The compound 4 showed highest score of -5.320918 greater than co-crystal showing two interactions with the residues Tyr 306 and one interaction with Phe 208 having hydrogen bonds of length 2.662 Å and 2.812Å respectively.

The SP docking for tubulin (1Z2B) with top 24 compounds selected from SP docking showed six best compounds (2, 4, 5, 10, 18 and 24) in comparison with co-crystal ligand (VLB). Among the six compounds docked with Tubulin (1Z2B) were shown in **Table 3**. The co-crystal ligand showed highest score of -3.506094 showing two strong interactions with the residues Thr 349 and Asn 329 having hydrogen bonds of length 2.818 Å and 3.853 Å.

The compound 2 showed highest score of -6.727805 greater than co-crystal showing strong interaction with the residues Asn 199 and Val151 having hydrogen bonds of length 2.001 Å and 1.682Å. The compound 24 showed highest score of -6.432191 greater than co-crystal showing strong interaction with the residues Ala 204 having hydrogen bonds of length 2.198 Å. The compound 4 showed the highest score of -5.927351 greater than co-crystal showing two interactions with the residues Phe 321 and one interaction with Asn 208 having hydrogen bonds of length 2.132 Å and 2.812 Å. The compound 5 showed highest score of -5.690095 greater than co-crystal showing two interactions with the residues Asn102 and one interaction with Asn 99 having hydrogen bonds of length 2.204Å and 1.440Å respectively.

XP Docking: The high scored bioactive compounds screened from SP docking for the entire four target proteins were now subjected to XP docking. In XP docking, highly scored active compounds were selected in comparison with corresponding co-crystal ligand (1T69-SHH and 1Z2B-VLB). Among the six compounds docked with Histone deacetylase (1T69) were shown in **Table 7**.

Among the top six compounds selected from SP docking compounds and showed four high scores and energy in XP docking for histone deacetylase (1T69) with co-crystal ligand (SHH). The co-crystal ligand showed highest score of-5.756641 showing two strong interactions with the same residue Asp 101 having hydrogen bonds of length 2.735 Å and 3.009 Å. The compound 5 showed highest score of -6.602465 greater than co-crystal showing strong interaction with the residues Tyr 306 and Phe 208 having hydrogen bonds of length 2.732 Å and 2.983 Å.

TABLE 6: SP DOCKING FOR TUMOR TARGET PROTEIN TUBULIN (1Z2B) WITH BIOACTIVE COMPOUNDS OF MEFrB

Tumor targets	Compound number	Glide score	Glide energy (Kcal / Mol)	Hydrogen bond interactions (DH…A)	Bond distance (Å)
Tubulin (1Z2B)	**Co-crystal (VLB)**	**-3.506094**	**-29.395245**	**(OH…O)Thr 349**	**2.818**
				(OH…O)Asn 329	**2.853**
	Compound 2	-6.727805	-30.855328	Asn 199 (OH...O)	2.001
				Val151 (NH…O)	1.682
	Compound 4	-5.927351	-26.041248	Phe 321(OH...O)	2.132
				Asn 208(NH...O)	2.812
	Compound 5	-5.690095	-38.596353	Asp 102(OH...O)	2.204
				Asn 99(NH...O)	1.440
	Compound 10	-5.568694	-34.622173	Asn 302(OH...O)	2.402
				Asp199 (NH...O)	2.188
	Compound 18	-5.330918	-31.641964	Asn 174(OH...O)	2.102
				Asn 177 (NH...O)	2.504
	Compound 24	-6.432191	-31.061938	Ala204 (OH….O)	2.198

The compound 24 showed the highest score of -6.210359 greater than co-crystal showing strong interaction with the residues Tyr 306 having hydrogen bonds of length 2.450Å, respectively. The compound 4 showed the highest score of -5.849041 greater than co-crystal showing strong interaction with the residues Tyr 306 and Phe 208 having hydrogen bonds of length 2.662 Å and 2.812 Å.

The XP docking for Tubulin (1Z2B) with top-six compounds selected from SP docking showed five best high score and energy in XP docking for Tubulin (1Z2B) in comparison with co-crystal ligand (VLB). Among the six compounds docked with Tubulin (1Z2B) were shown in **Table 8**. The co-crystal ligand showed highest score of -3.506094showing two strong interactions with the residues Thr 349 and Asn 329 having hydrogen bonds of length 2.818 Å and 2.853 Årespectively. The compound 24 showed highest score of -6.860716 greater than co-crystal showing strong interaction with the residues Asn 206, Ala174, and Val17 having hydrogen bonds of length 2.021Å, 2.135 Å and 1.766 Å respectively. The compound 4 showed highest score of -4.423304 greater than co-crystal showing strong interaction with the residues Phe 351, Asn 329, and Asn 249 having hydrogen bonds of length 3.050 Å, 2.916 Å and 2.997 Å respectively. The compound 5 showed highest score of -3.930545 greater than co-crystal showing two interactions with the residues Asn 329 and one interaction with Asn 249 having hydrogen bonds of length 3.125Å, 2.891 and 3.456 Å respectively.

TABLE 7: XP DOCKING FOR TUMOR TARGET PROTEIN HISTONE DEACTYLASE (1T69) WITH BIOACTIVE COMPOUNDS OF MEFrB

Tumor targets	Compound number	Glide score	Glide energy (Kcal / Mol)	Hydrogen bond interactions (DH…A)	Bond distance (Å)
Histone deactylase (1T69)	**Co-crystal (SHH)**	**-5.756641**	**-35.742488**	**Asp101(OH…O)**	**2.735**
				Asp 101(NH…O)	**3.009**
	Compound 2	-7.616970	-35.875466	Tyr 306(OH...O)	2.917
				Gly 151(NH…O)	3.074
	Compound 4	-5.849041	-33.052920	Tyr 306(OH...O)	2.662
				Phe 208(NH...O)	2.812
	Compound 5	-6.602465	-35.914890	Tyr 306(OH...O)	2.732
				Phe 208(NH...O)	2.983
	Compound 24	-6.210359	-30.8575466	Tyr306 (OH….O)	2.450

TABLE 8: XP DOCKING FOR TUMOR TARGET PROTEIN TUBULIN (1Z2B) WITH BIOACTIVE COMPOUNDS OF MEFrB

Tumor targets	Compound number	Glide score	Glide energy (Kcal / Mol)	Hydrogen bond interactions (DH…A)	Bond distance (Å)
Tubulin (1Z2B)	**Co-crystal (VLB)**	**-3.506094**	**-29.395245**	**(OH…O)Thr 349**	**2.818**
				(OH…O)Asn 329	**2.853**
	Compound 4	-4.423304	-30.851479	Phe 351(OH…O)	3.050
				Asn 329(NH…O)	2.916
				Asn 249(NH…O)	2.997
	Compound 5	-3.930545	-30.183197	Asn 329(NH…O)	3.125
				Asn 329(NH…O)	2.891
				Asn 249(NH…O)	3.456
	Compound 10	-4.36700	28.045210	Asp 98 (OH…O)	1.540
				Asn 101 (NH…O)	2.408
	Compound 18	-3.76100	-49.76400	Asn 101 (NH…O)	2.265
	Compound 24	-6.860716	-23.287357	Asn 206 (NH…O)	2.021
				Ala 174 (NH…O)	2.135
				Val 177 (NH…O)	1.766

The compound 10 showed the highest score of -4.36700 than co-crystal showing two interactions with the residues Asp 98 and one interaction with Asn 101 having hydrogen bonds of length 1.540Å and 2.408 Å respectively. The compound 18 showed highest score of -3.76100 greater than co-crystal showing one interaction with the residues Asn 101 having hydrogen bonds of length 2.265 Å, respectively. The compound 28 showed highest score of -3.601280 greater than co-crystal showing two interactions with the residues Asp 98 and one interaction with Asn 249 and Asn249 having hydrogen bonds of length 2.964Å and 3.084 Å respectively.

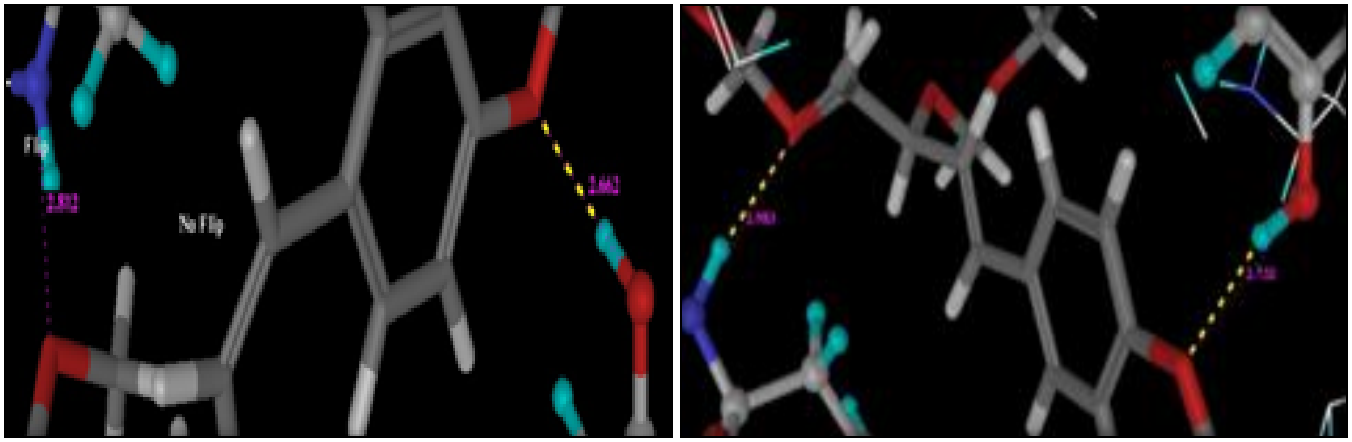

1T69 (Compound 4) **1T69 (Compound 5)**

FIG. 8: XP DOCKING OF COMPOUND 4 AND 5 WITH HISTONE DEACTYLASE (1T69)

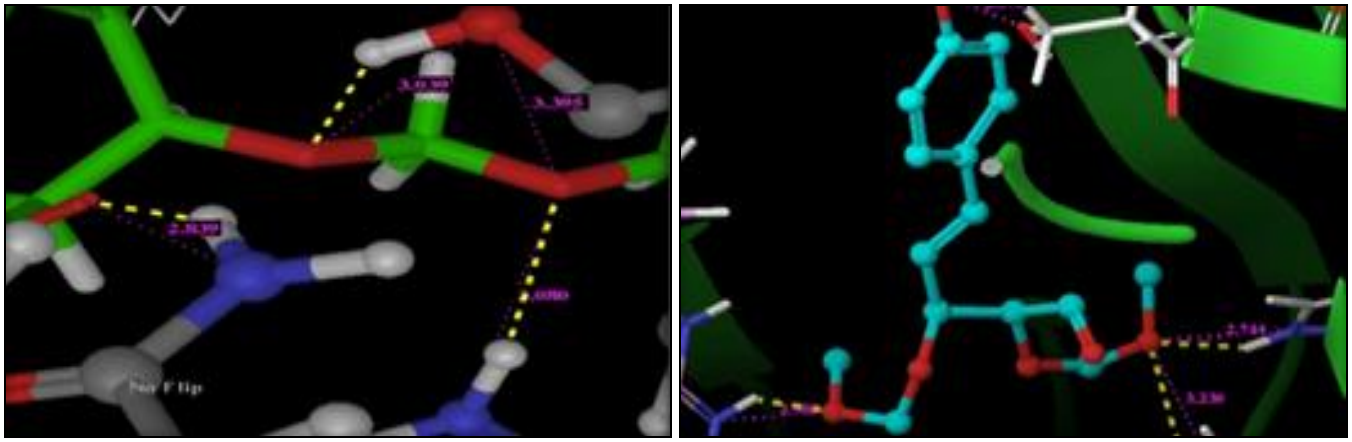

1Z2B (compound 4) **1Z2B (compound 5)**

FIG. 9: XP DOCKING OF COMPOUND 4 AND 5 WITH TUBULIN (1Z2B)

Induced Fit Docking: Induced fit docking were used to perform an interactive study, where more number of poses can be generated for a single ligand that can be docked with the target receptor molecule. From the results of XP docking, highly scored compounds from tumorigenic and microbial targets were subjected to induced fit docking. The present study on XP docking for bioactive compounds on tumorigenic targets (1T69 and 1Z2B) showed high score and interactions for the seven compounds 2, 4, 5, 10, 18 and 24.

TABLE 9: INDUCED FIT DOCKING OF TUMOR TARGET PROTEIN HISTONE DEACTYLASE (1T69) WITH THE BIOACTIVE COMPOUND OF MEFrB

Tumor target (1T69)	Pose Number	Glide score	Glide energy (Kcal / Mol)	Hydrogen bond Interactions (DH…A)	Bond distance (Å)
Co-crystal (SHH)	**Pose 1**	**-4.547854**	**-42.202789**	**Asp178(OH…O)**	**2.660**
				Asp 267(NH…O)	**2.769**
				Tyr 306(OH…O)	**2.810**
Compound 4	Pose 1	-6.094091	-45.473108	Tyr 306(OH...O)	2.783
				Lys 33 (NH...O)	3.198
				Hie 180(NH...O)	2.942
	Pose 2	-5.845370	-45.878405	Gly 305 (NH...O)	3.003
	Pose 3	-5.798657	-45.301232	Tyr 306(OH...O)	3.137
				Tyr 306(OH...O)	2.790
				Asp 267(OH…O)	3.084
Compound 5	Pose 1	-6.762940	-42.202323	Gly 305(NH...O)	3.218
				Trp 141(NH...O)	2.721
	Pose 2	-6.523717	-43.057300	Hie 180(NH...O)	2.977
	Pose 3	-5.451383	-34.974048	Hie 143(NH...O)	2.938

So, these highly scored compounds selected from both the targets were used to perform induced-fit docking with their corresponding targets. The induced-fit docking results for the highly scored compounds (4 and 5) with their corresponding tumorigenic and microbial targets were depicted in the following **Tables 9**.

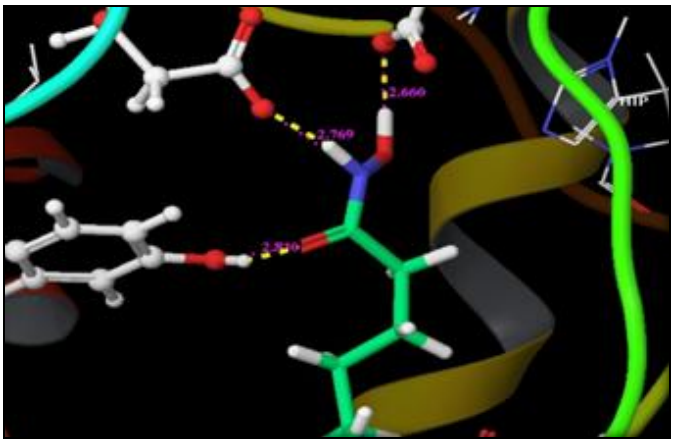

FIG. 10: DOCKING OF CO-CRYSTAL LIGAND (SHH) WITH HISTONE DEACTYLASE (1T69)

In induced-fit docking, each compound was obtained with 3 poses and the best pose was pictorially represented. The table shows the induced fit docking results for a tumorigenic target-Histone deacetylase (1T69) with highly scored compounds (4 and 5) of three poses each. The co-crystal (SHH) showed a score of -4.547854 by showing strong interactions with the residue Asp178, Asp 267 and Tyr 306 having hydrogen bonds of length 2.660 Å, 2.769 and 2.810 Å respectively **Fig. 10**.

The compound 4 was obtained with 3 poses and all the 3 poses showed the highest score compared to the co-crystal ligand. The best pose showed the highest score of -6.094091 and strong interactions with the residue Tyr 306, Lys 33 and His 180 having hydrogen bonds of length 2.783Å, 3.198 Åand 2.942Å. The compound 5 was obtained with 3 poses, and all the 3 poses showed highest score compared to the co-crystal ligand. The best pose showed the highest score of -6.762940 and strong interactions with the residue Gly 305 and Trp 141 having hydrogen bonds of length 3.218Å and 2.721Å respectively **Fig. 11**.

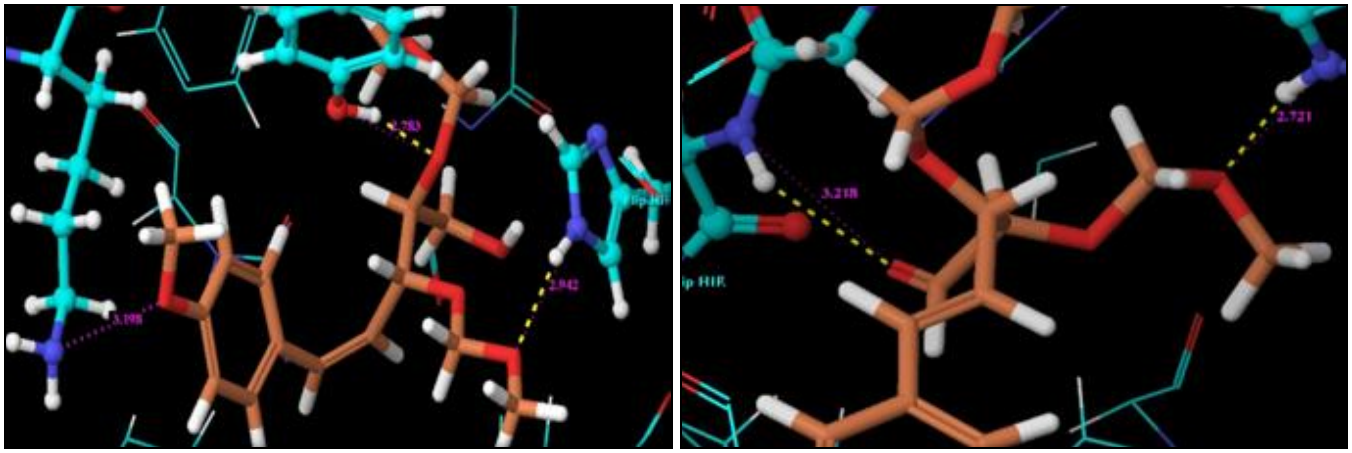

FIG. 11: DOCKING OF COMPOUND 4 AND 5 WITH HISTONE DEACTYLASE (1T69)

Table 10 shows the induced fit docking results for the tumorigenic target - Tubulin (1Z2B) with highly scored compounds (4 and 5) of three poses each. The co-crystal (VLB) showed a score of -3.686134 and strong interactions with the residue Lys 336 having hydrogen bonds of length 2.758 Å **Fig. 12**. The compound 4 was obtained with 3 poses and all the 3 poses showed highest score compared to the co-crystal ligand. The best pose showed the highest score of -5.245243 and 1 interaction with the residue Asn 329, 3 interactions with same residue Lys 336 and 1 interaction with residue Gly 350 having hydrogen bonds of length 2.935 Å, 2.771 Å, 2.983 Å,2.982 Å, and 2.814 Å respectively **Fig. 13**.

The compound 5 was obtained with 3 poses, and all the 3 poses showed the highest score compared to the co-crystal ligand. The best pose showed the highest score of -4.614675 and 2 strong interactions with same residue Lys 336 and 1 interaction with the residue Asn 329 having hydrogen bonds of length 2.885Å, 2.780 Å and 2.721 Å respectively **Fig. 13**.

TABLE 10: INDUCED FIT DOCKING OF TUMOR TARGET PROTEIN TUBULIN (1Z2B) WITH THE BIOACTIVE COMPOUND OF MEFrB

Tumor target (1T69)	Pose Number	Glide score	Glide energy (Kcal / Mol)	Hydrogen bond Interactions (DH…A)	Bond distance (Å)
Co-crystal (VLB)	**Pose 1**	**-3.686134**	**-32.534403**	**Lys 336(NH…O)**	**2.758**
Compound 4	Pose 1	-5.245243	-34.762822	Asn 329(NH...O)	2.935
				Lys 336 (NH...O)	2.771
				Lys 336 (NH...O)	2.983
				Lys 336 (NH...O)	2.982
				Gly 350(OH…O)	2.814
	Pose 2	-4.770638	-35.405276	Asn 329(NH...O)	3.404
				Lys 336 (NH...O)	2.703
				Lys 336 (NH...O)	2.880
				Gly 350(OH…O)	2.844
	Pose 3	-4.226431	-33.514821	Lys 336 (NH...O)	2.955
				Lys 336 (NH...O)	3.079
				Gly 350(OH…O)	2.859
Compound 5	Pose 1	-4.614675	-35.631538	Lys 336 (NH...O)	2.885
				Lys 336 (NH...O)	2.780
				Asn 329(NH...O)	3.226
	Pose 2	-4.567160	-32.091455	Lys 336 (NH...O)	3.064
				Lys 336 (NH...O)	2.848
	Pose 3	-4.386168	-34.784741	Thr 349(OH...O)	2.922
				Lys 336 (NH...O)	3.034

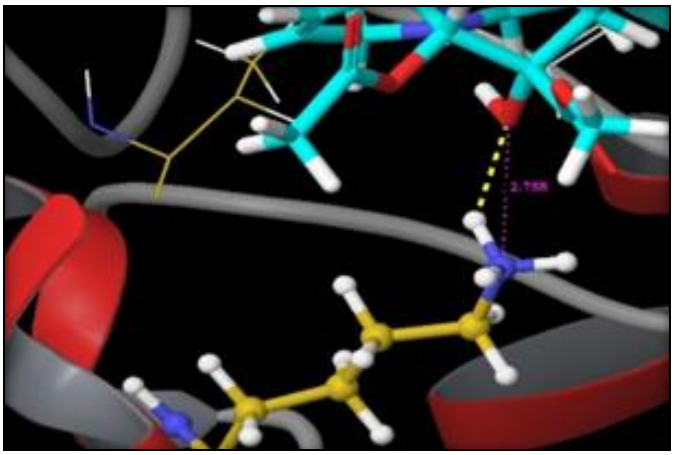

FIG. 12: DOCKING OF CO-CRYSTAL LIGAND (VLB) WITH TUBULIN (1Z2B)

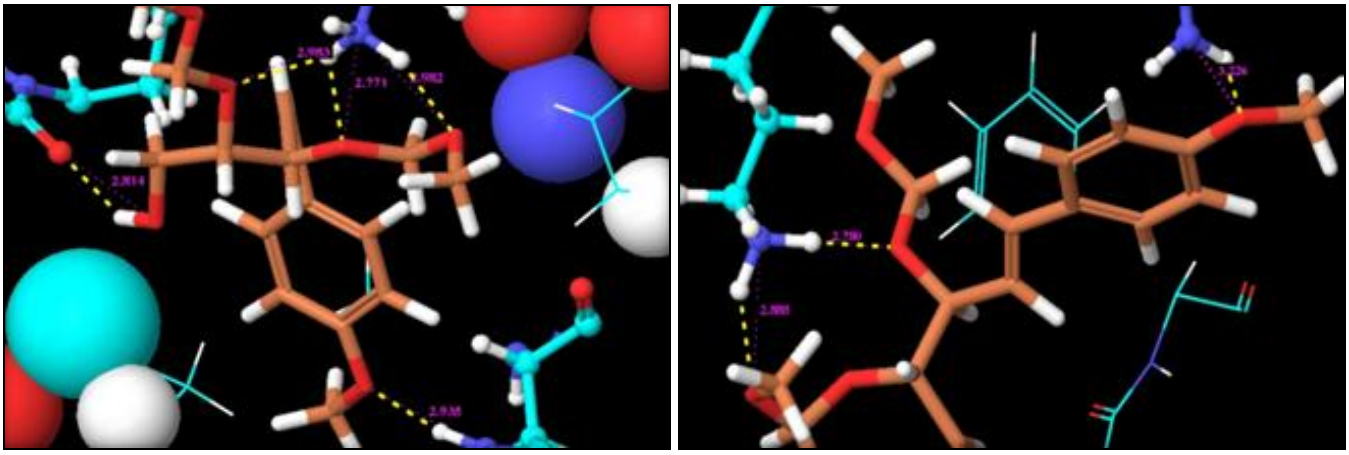

FIG. 13: DOCKING OF COMPOUND 4 AND 5 WITH TUBULIN (1Z2B)

Prediction of ADME Properties: Nearly 40% of drug candidates fail in clinical trials due to poor ADME properties. These late-stage failures contribute significantly to the skyrocketing cost of

new drug development. The ability to detect problematic candidates early will dramatically reduce the amount of wasted time and resources, and streamline the overall development process [6].

According to Lipinski's rule of five" is a rule of thumb to evaluate drug-likeness or determine if a chemical compound with a certain pharmacological or biological activity that would make it a likely orally active drug in humans. The rule describes molecular properties important for a drug's pharmacokinetics in the human body including their absorption, distribution, metabolism, and excretion (ADME). Over the past decade, ADME property evaluation has become one of the most important issues in the process of drug discovery and development. Since *in-vivo* and *in-vitro* evaluations are costly and laborious, *in-silico* techniques had been widely used to estimate ADME properties of chemical compounds.

It is gaining acceptance as a useful assessment tool for early identification of likely drug candidate failures. *In-silico* prediction of ADME properties for the selected plant constituents was performed using the program QikProp, and the results were presented in **Table 11**.

TABLE 11: PREDICTION OF ADME PROPERTIES OF THE BIOACTIVE COMPOUNDS 4 AND 5

S. no.	List of properties	Highly scored plant constituent	
		(Z)-(2S,3S)-2,3 bis [(methoxy -methyl)oxy] -5-(4-methoxyphenyl)pent-4-enol	(E)-(2S,3S)-2,3-bis [(methoxymethyl)oxy]-5-(4-methoxyphenyl) pent-4-enal
1	Molecular formula	$C_{16}H_{24}O_6$	$C_{16}H_{22}O_6$
2	Molecular weight (130 to 725)	312	310
3	Donor HB (0.0 to 6.0)	1.000	0.000
4	Acceptor HB (2.0 to 20.0)	9.250	9.550
5	Number of rotatable bonds (0 to 15)	12	11
6	QPlogs (-6.5 to 0.5)	-1.236	-0.012
7	Qplog Po/w (-2.0 to 6.5)	1.704	1.050
8	QplogBB (-3.0 to 1.2)	-0.514	-0.554
9	%Human oral absorption (>80%-High <25%-Poor)	100 (High)	96 (High)
10	Rule of five	0	0

Here, the set of linear descriptors are applied on the highly scored best bioactive plant compounds and tested for Lipinski's rule of five to evaluate drug-likeness. The ADME property prediction on these highly scored compounds (4 and 5) showed that they do not violate any of the rules for drug solubility and permeability estimation. The tumorigenic target histone deacetylase (1T69) and tubulin (1Z2B) is a crucial factor in carcinogenesis, as well as a promising target for the development of anticancer drugs and therapies. The rise of multidrug resistance of many human pathogens necessitates the development of new therapeutic agents against microbial target deacetoxy C synthase (1W2N) and pantothenate kinase (1SQ5).

From the results of ADME calculation the compound 4[(Z)-(2S,3S)-2, 3 bis [(methoxy -methyl)oxy] -5-(4-methoxyphenyl)pent-4-enol] and the compound 5[(E)-(2S, 3S)-2, 3-bis [(methoxy methyl) oxy]-5-(4-methoxyphenyl) pent-4-enal] may be used as an anticancer agent to treat the diseases like cancer. A novel approach for assessing prostate cancer initiation and disease progression suggests a molecular target tubulin for therapeutic intervention in prostate cancer and perhaps other forms of cancer by catalyzing the diverse tubulin posttranslational modifications [7].

The HDAC inhibitors therapeutic agents to modulate a wide variety of cellular functions, transcriptional activity in cells, cell cycling, angiogenesis, apoptosis and differentiation which are key components of tumor proliferation. HDAC inhibitors may improve the efficacy of existing cancer therapies. The reported the molecular docking studies of some novel hydroxamic acid derivatives with human histone deacetylase. The reported the molecular docking analysis of cembrenoids with tubulin in order to assess the potential of tubulin-binding of the cytotoxic agents. These above results also confirmed the anti-tumorigenic role of MEFrB [8].

The GLIDE docking analysis of 24 bioactive compounds from the medicinal plant - *Ficus racemosa* showed good interaction with all the two targets. The binding sites of the compounds were found to be in close proximity to the binding site of its co-crystal ligand. It was interesting to observe that even though the core structure of all the compounds was the same, the degree of interaction and binding site were found to be different. The compounds (4 and 5) identified from methanolic extract of *Ficus racemosa* bark showed highest glide score, glide energy and interactions compared to the other compounds.

The compounds identified in GC- MS analysis was subjected to SP docking against the cancer target proteins histone deacetylase and tubulin with co-crystal interaction of SHH and VLB respectively. Out of 24 compounds, only 2, 4, 5, 10, 18 and 24 compounds were found to be successful in SP docking and these compounds were selected for XP docking. In XP and induced fit docking showed high score for only two compounds [(Z)-(2S, 3S)-2, 3 bis [(methoxymethyl) oxy] -5-(4-methoxyphenyl) pent-4-enol] and [(E)-(2S, 3S)-2, 3-bis [(methoxymethyl) oxy]-5-(4-methoxyphenyl) pent-4-enal]. ADME properties of these two compounds in QikProp program showed drugable property, solubility, and permeability and also obeyed Lipinski's rule.

CONCLUSION: It can be concluded that the *in-silico* SP, XP and IF docking studies revealed the presence of two compounds namely [(Z)-(2S,3S)-2,3 bis [(methoxymethyl)oxy] -5-(4-methoxy phenyl)pent-4-enol] and [(E)-(2S, 3S)-2, 3-bis [(methoxymethyl) oxy]-5-(4-methoxyphenyl) pent-4-enal] of MEFrB may be recommended as anti-tumorigenic agent to the individual suffering from oxidative degenerative diseases.

ACKNOWLEDGEMENT: The authors acknowledge the Avinashilingam Institute of Home Science and Higher Education for Women, Coimbatore, India for providing the necessary amenities.

CONFLICT OF INTEREST: The authors declared that there is no conflict of interest.

REFERENCES:

1. Sakhanda IV and Kosyachenko KL: Assortment of herbal medicines of the treatment of cardiovascular diseases. Wiad Lek 2018; 71(5): 1104-08.
2. Eshwarappa RSB, Iyer S, Subaramaihha SR, Richard SA and Dhananjaya BL: Antioxidant activities of *Ficus glomerata* (moraceae) leaf gall extracts. Pharmacognosy Res 2015; 7(1): 114-20.
3. Raaman N: Phytochemical Techniques, New Publishing Agency, New Delhi 2006: 19(24): 32-40.
4. Iyengar MA: Study of crude drugs, Manipal Power Press, Manipal, India, Edition 8th, 1995: 2.
5. Siddiqui AA and Ali M: Practical Pharmaceutical Chemistry, CBS Publishers and Distributors, New Delhi, Edition 1st, 1997: 126-31.
6. Kaitin KI: Deconstructing the drug development process: The new face of innovation. Clin Pharmacol Ther 2010; 87(3): 356-61.
7. Audia JE and Campbell RM: Histone modifications and cancer, Cold Spring Harbor Laboratory Press, 2016; 3(1): 1-33.
8. Eckschlager T, Plch J, Stiborova M and Hrabeta J: Histone Deacetylase inhibitors as anticancer drugs. International Journal of Molecular Sciences 2017; 18: 1414.

How to cite this article:
Poongothai A and Annapoorani S: GC- MS analysis and *in-silico* docking analysis of methanolic extract of *Ficus racemosa* bark. Int J Pharm Sci & Res 2019; 10(11): 5179-93. doi: 10.13040/IJPSR.0975-8232.10(11).5179-93.